Peng-Long Qiu, Xin-Mei Hou* and Kuo-Chih Chou

Morphology-controlled Synthesis of Hexagonal AlN Whiskers by Direct Nitridation of Aluminum and Alumina Mixture

Abstract: Hexagonal 1D AlN whiskers were synthesized by direct nitridation of aluminum and alumina. The effect of the atmosphere was investigated based on thermodynamic calculation. A green body compacting alumina with different particle size in between 44–420 μm in graphite crucible was found to be favorable for the large-scale synthesis of AlN at 1650 °C for 3 h in flowing nitrogen atmosphere. XRD result indicated that hexagonal AlN phase with high purity has been successfully synthesized. SEM and TEM analysis indicated that the whiskers possessed uniform morphology with 100–200 nm in diameter and length up to microns. The formation mechanism was further proposed based on the experimental results.

Keywords: aluminum nitride whiskers, direct nitriding method, morphology

PACS® (2010). 61.46.+w

***Corresponding author: Xin-Mei Hou:** Department of Physical Chemistry, School of Metallurgical and Ecological Engineering, University of Science and Technology Beijing, Beijing 100083, China. E-mail: houxinmei@ustb.edu.cn

Peng-Long Qiu, Kuo-Chih Chou: Department of Physical Chemistry, School of Metallurgical and Ecological Engineering, University of Science and Technology Beijing, Beijing 100083, China

1 Introduction

Aluminum nitride (AlN) has aroused great interest due to its high thermal conductivity, good electrical resistance, low dielectric constant and low thermal expansion coefficient, matching that of silicon [1–7]. Recently 1D AlN nanostructures, such as nanowhiskers, nanorods and nanobelts have attracted much attention because their perfect or near perfect crystal structures are supposed to have higher thermal conductivity than ordinary polycrystalline AlN ceramics [8]. In addition, they could provide better reinforcement in the composites [9]. AlN whiskers or fibers have been used to optimize the thermal properties of polymer composites for electronic packaging [10].

Various synthetic routes have been development to fabricate AlN whiskers, including combustion synthesis, vapor-solid (VS) process, anodic porous alumina template, directly nitriding aluminum powders under ammonia/nitrogen with or without a catalyst, carbothermal reduction and nitridation of electrospun precursor fibers or solid solution precursors, direct sublimation method [11–22] and so on. In this study, AlN whiskers with large scale were successfully obtained by direct nitridation of the mixture of Al and Al_2O_3 with different particle size. AlN phase with high purity was produced by controlling the reaction atmosphere. The products were characterized by XRD, FE-SEM and TEM. The synthesis mechanism was proposed to interpret the formation. Compared with the other synthetic methods, the fabricated technique used in this work is suitable for generating whiskers with uniform morphology and possesses the virtues including simplicity, low cost and absence of template.

2 Experimental

Al supplied by Sinopharm with purity of 99.5 wt% and Al_2O_3 obtained from Sinopharm with purity of 99.5 wt% were used as starting material to synthesize AlN whiskers. The average particle size of Al was 74 μm. The purpose of adopting Al_2O_3 in the experiment was to control the reaction rate of nitridation of Al. In the experiment, Al_2O_3 powder with average particle size of 420, 150 and 44 μm were adopted. The mixture of Al and Al_2O_3 with the mole ratio of 9:1 was pressed into a bar sample with 60 mm × 7 mm × 4 mm in size. The schematic diagram of the experimental setup is shown in Fig. 1. The sample was put into a graphite crucible and then heated up 1650 °C for 3 h in two stages. First stage, the mixture was heated to 700 °C for 1 h in nitrogen. Subsequently, the samples were heated at 1650 for 3 h in flowing nitrogen atmosphere with the flow rate of 2 L/min. When the furnace was cooled naturally to 500 °C, nitrogen was stopped and gray-white whiskers were obtained.

The phases were identified by X-ray diffraction (XRD; M21XVHF22, MAC Science, Yokohama, Japan) using Cu Kα

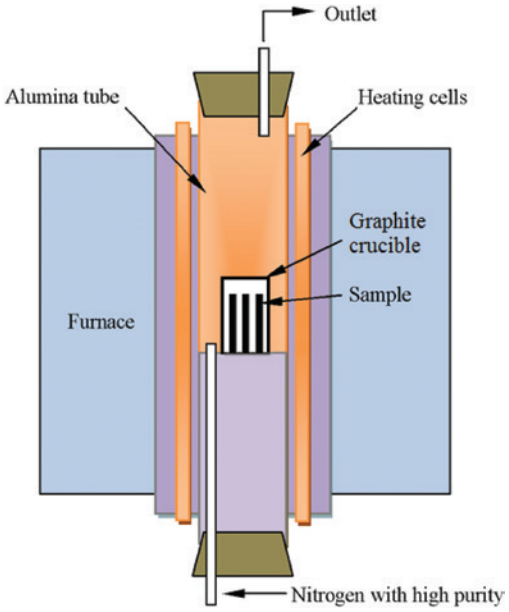

Fig. 1: The schematic diagram of the reaction equipment

radiation (40 KV, 20 mA, $\lambda = 1.5406$ Å) in the angular 10–100° with the scan speed of 2 °/min. The morphology of the fibers was examined by thermal field emission scanning electron microscopy (FE-SEM; ZEISS SUPRATM 55, Germany) and transmission electron microscopy (TEM, HITACHI H8100, Hitachi, Japan). High resolution electron microscopy (HRTEM, JEM 2010, Joel Ltd., Japan) operating at 200 kV was used to characterize the phase and crystal morphology of the products.

3 Results and discussion

3.1 Thermodynamic calculation

In this experiment, Al_2O_3 was used to control the nitridation rate of Al with N_2. Meanwhile, Al_2O_3 increased the chance of oxygen contamination of Al and AlN, which is known to negatively influence AlN crystal properties [23]. Therefore Al-O-N system was involved during the formation of AlN whiskers in the experiment. In the following section, the possible reactions involved and the underlying thermodynamic principle will be discussed.

In Al-O-N system, the possible solid phases are AlN, Al_3O_3N spinel phase [24] and Al_2O_3. Al-containing gases are Al(g), Al_2O(g), AlO(g) and AlO_2(g). It is known that the melt point of Al is 661 °C and thus it was in the liquid phase in the experiment. The possible reactions together with the standard reaction Gibbs free energy in the system are shown in Table 1 [25].

Table 1: The reactions and related thermodynamic data in Al-O-N system

Equations		The standard reaction Gibbs free energies ($J \cdot mol^{-1}$)
$2Al(l) + \frac{1}{2}O_2(g) = Al_2O(g)$	(1)	$\Delta G_r^\theta = -192308 - 41.65T$
$Al(l) + \frac{1}{2}O_2(g) = AlO(g)$	(2)	$\Delta G_r^\theta = 14640 - 55.69T$
$Al(l) + O_2(g) = AlO_2(g)$	(3)	$\Delta G_r^\theta = -619982 + 70.60T$
$2Al(l) + O_2(g) = Al_2O_2(g)$	(4)	$\Delta G_r^\theta = -431143 + 23.32T$
$Al(l) + \frac{1}{2}N_2(g) = AlN(s)$	(5)	$\Delta G_r^\theta = -328856 + 116.97T$
$Al(g) + \frac{1}{2}N_2(g) = AlN(s)$	(6)	$\Delta G_r^\theta = -644286 + 233.55T$
$AlO(g) + \frac{1}{2}N_2(g) = AlN(s) + \frac{1}{2}O_2(g)$	(7)	$\Delta G_r^\theta = -380452 + 181.93T$
$AlO_2(g) + \frac{1}{2}N_2(g) = AlN(s) + O_2(g)$	(8)	$\Delta G_r^\theta = -230271 + 110.84T$
$Al_2O(g) + N_2(g) = 2AlN(s) + \frac{1}{2}O_2(g)$	(9)	$\Delta G_r^\theta = -484061 + 287.31T$
$Al_2O_2(g) + N_2(g) = 2AlN(s) + O_2(g)$	(10)	$\Delta G_r^\theta = -235245 + 217.10T$

As shown in Table 1, the standard reaction Gibbs free energies of the above Eqs. (1)–(8) are negative in the temperature range of 1500 to 1650 °C. While the standard reaction Gibbs energies of Eqs. (9)–(10) are positive at high temperature, indicating they cannot happen under the standard condition thermodynamically. However, the partial pressures of oxygen can be very low resulting in negative Gibbs energies of these reactions. To obtain low oxygen partial pressure, carbon can be added because it will react with oxygen by following reaction:

$$C + \frac{1}{2}O_2(g) = CO(g) \tag{11}$$

When the equation reaches equilibrium, $\Delta G_{(P,T)} = 0$. The following equation can be obtained:

$$\lg\left(\frac{p_{O_2}}{p^\theta}\right) = 2\lg\left(\frac{p_{CO}}{p^\theta}\right) - 8.965 - \left(\frac{11972}{T}\right) \tag{12}$$

According to Eq. (12), the oxygen partial pressure is much smaller than that of CO at high temperature, indicating that the extra low oxygen partial pressure can be obtained by adding carbon. In the experiment, the graphite crucible was used to control the oxygen partial pressure. In addition, Eqs. (7)–(10) can easily proceed forward because of consumption of oxygen by carbon.

3.2 Phase and microstructure characterization

The XRD pattern of as-prepared gray-white product was shown in Fig. 2. All of the reflection peaks as d-spacings of 3.4102, 2.1762, 2.0747, 1.6844, 1.2556 Å can be indexed

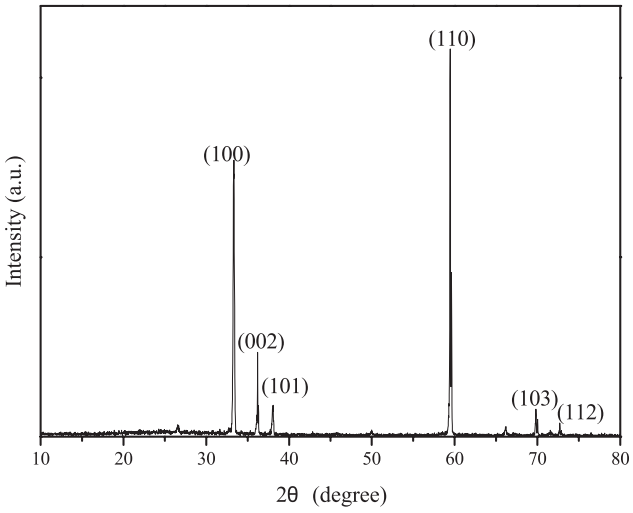

Fig. 2: XRD pattern of AlN whiskers

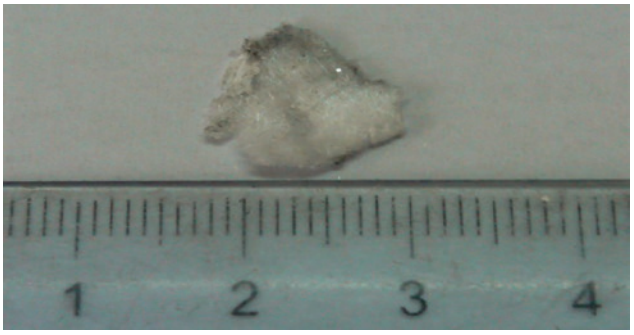

Fig. 3: The digital photo of obtained AlN whiskers

as hexagonal AlN ((002), (100), (101), (004), (110)) (JCPDS card No. 25-1133), indicating that the gray-white product is h-AlN [18]. No other noticeable peaks introduced by impurities are observed in the XRD patterns.

Large scale gray-white whiskers were formed on the surface of the sample. Fig. 3 is the digital photo of the gray-white whiskers. The length of the synthesized whiskers was up to microns. Fig. 4 shows the microstructure of synthesized AlN at different magnifications. It can be seen that the synthesized AlN was long and straight filaments with diameters of 100–200 nm on average. Two typical morphologies of AlN whiskers can be observed. One is the cross-sectional views were hexagonal in shape and with growth steps at its side as shown in Fig. 5 (the inset shows a magnified image). The other is the cross-sectional views were hexagonal in shape but with smooth surface (Fig. 6). More details about the structure of as-obtained whiskwers were investigated by TEM together with the result of high resolution transmission electron

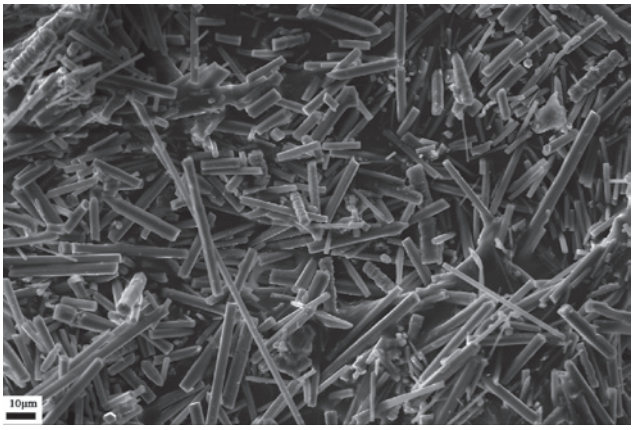

Fig. 4: SEM image of synthesized AlN whiskers

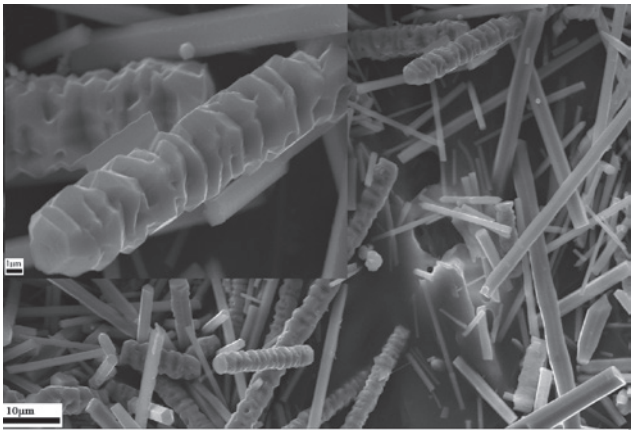

Fig. 5: SEM images of AlN whiskers with growth step at different magnification

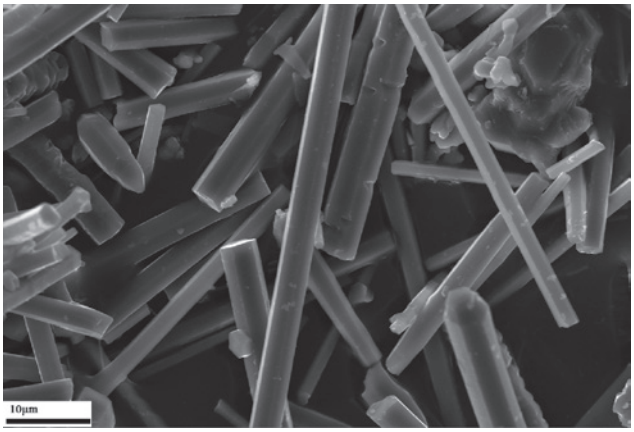

Fig. 6: SEM image of AlN whiskers with smooth surface

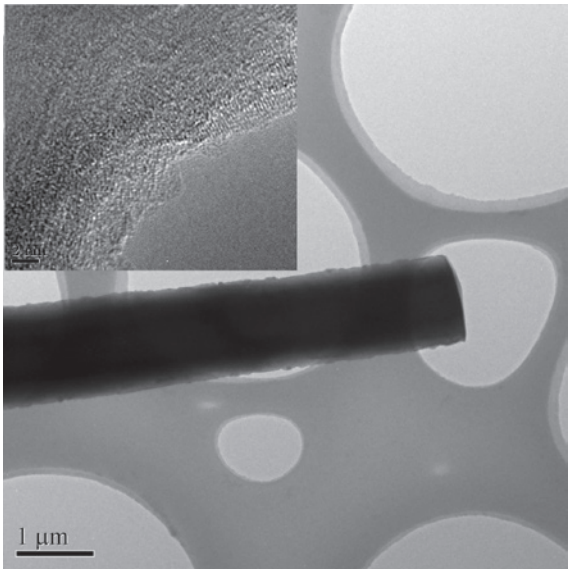

Fig. 7: TEM and HRTEM images of the synthesized AlN whiskers

microscopy (HRTEM) indicated that the whiskers have a hexagonal polycrystalline structure (Fig. 7).

3.3 Reaction mechanism

VS (vapor-solid) and VLS (vapor-liquid-solid) are two well known mechanisms for the formation of 1D nanomaterials [26]. In the VLS mechanism a liquid droplet will be initially formed, and then reactant molecules in the vapor are transported by diffusion to the liquid-solid interface, where precipitation occurs and with crystal growth the droplet is detached from the substrate. During the cooling stage the liquid droplet forms a nodule at the top of the whisker, which is considered a characteristic morphology of the VLS mechanism. In the micrographs of the AlN fibers observed in this study, no nodule was observed at the ends of those whiskers. As shown in Figs. 5 and 6, the top of AlN is well developed, indicating that AlN whiskers were mainly nucleated by VS mechanism. The distinction of AlN whiskers morphologies can be explained from their growth space and supersaturation. According to the Burton-Carbrera-Frank (BCF) theory [27], the crystal nucleation and growth from the vapor mainly depends on the supersaturation ratio (p/p_e), where p and p_e are the actual and equilibrium pressure. As is known, on any plane, growth occurs at kink sites at which the attachment energy is equal to the mean binding energy per atom of bulk. Kink sites are plentiful on high energy plane and the growth rate is directly proportional to the supersaturation. At high supersaturation kink sites are also freely nucleated on low energy planes so that growth is again unimpeded. At lower supersaturation the growth rate of low energy planes becomes limited by the nucleation rate of kink sites. High energy planes then grow out and a crystal habit develops which is determined by the impeded growth rates of the low energy planes.

In this research, proximity to substrate surface, there is less growth space and higher supersaturation. Far from substrate surface, there is larger growth space and lower supersaturation. As the {0001}plane is known to be the preferential crystallographic plane for HCP crystals, AlN whishers grow with the {0001}plane as growth plane and have hexagonal cross section. The growth schematic diagram of AlN whiskers is illustrated in Fig. 8. According to previous reports, the nitridation of Al can start at a temperature as low as 550 °C, which is even lower than the melting point of Al [28]. The tiny AlN particles formed at lower temperature could act as seeds. When the temperature goes up, Al-containg gases such as Al_2O, AlO etc. were formed because oxygen as impurity existed in the notrogen. Al vapor and Al-containg gases becomes more available locally around the particles at high temperature, these gases have the tendency to deposit on the {0001}plane, where the growth energy is lower than other sites to form AlN whiskes. The deposition of AlN will grow into the preferred hexagonal shape to minimize the whole energy of the system and has smooth surface as shown in Fig. 7. In additon, it has been reported that the AlN whiskers formed by the VS mechanism contained a large

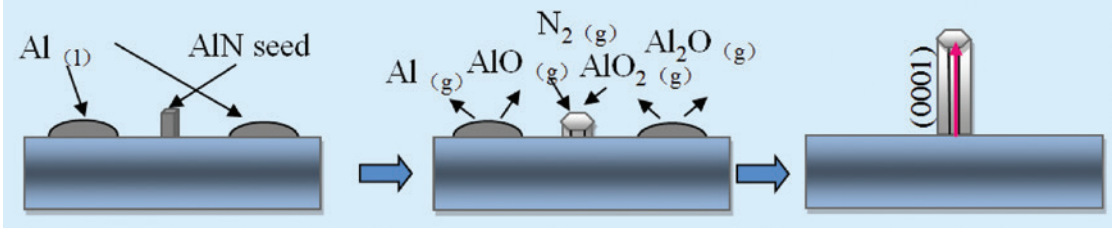

Fig. 8: The growth mechanism of AlN whiskers

number of stacking faults durinng the process of growth [29]. In this work, some AlN whiskers have dislocations on them, so they would grow via the spiral growth mechanism and made growth steps on their side as shown in Fig. 5.

4 Conclusion

1D hexagonal AlN whiskers were successfully fabricated by direct nitridation of the mixture of Al and Al_2O_3 with different particle size. It was found to be favorable for the large-scale synthesis of AlN whiskers with high purity at 1650 °C for 3 h in flowing nitrogen atmosphere. The morphology of the obtained AlN was uniform and mainly had hexagonal cross section with diameters of 100–200 nm on average and lengths up to microns. The formation of AlN was interpreted by VS mechanisms with important atmosphere effect.

The authors express their appreciation to the National Nature Science Foundation of China (No. 51104012) and the Fundamental Research Funds for the Central Universities (No. FRF-TP-12-024A) for their financial support.

Received: September 9, 2013. Accepted: October 21, 2013.

References

[1] H. Kitagawa, Y. Shibutani, S. Ogata, *Model. Simul. Mater. Sci.*, **3**(4) (1995) 521–531.
[2] Y. Goldberg, Wiley, New York, 2001, pp. 31–47.
[3] N. Kuramoto, H. Taniguchi, I. Aso, *Am. Ceram. Soc. Bull.*, **68**(4) (1989) 883–887.
[4] Y. Sun, J. Y. Li, Y. Tan, L. Zhang, *J. Alloy. Compd.*, **471**(1–2) (2009) 400–403.
[5] J. C. Kuang, C. R. Zhang, X. G. Zhou, Q. C. Liu, C. Ye, *Mater. Lett.*, **59**(16) (2005) 2006–2010.
[6] S. M. Bradshaw, J. L. Spicer, *J. Am. Ceram. Soc.*, **82**(9) (1999) 2293–2300.
[7] J. Liu, X. Zhang, Y. J. Zhang, R. R. He, J. Zhu, *J. Mater. Res.*, **16**(11) (2001) 3133–3138.
[8] P. G. Caceres, H. K. Schmid, *J. Am. Ceram. Soc.*, **77**(4) (1994) 977–983.
[9] S. M. L. Sastry, R. J. Lederick, T. C. Peng, *J. Metal.*, **40**(9) (1988) 11–13.
[10] L. M. Sheppard, *Am. Ceram. Soc. Bull.*, **69**(11) (1990) 1801–1812.
[11] J. Jia, Y. J. Zhang, Y. Q. Xiao, L. Zhao, *Chin. Ceram.*, **48**(10) (2012) 58–61.
[12] W. Wang, T. Xue, Z. H. Jin, G. J. Qiao, *Mater. Res. Bull.*, **43**(4) (2008) 939–945.
[13] L. Y. Wang, L. Zhang, *Powder Metall. Ind.*, **18**(3) (2008) 42–46.
[14] X. Y. Li, T. Qiu, C. Y. Shen, *J. Chin. Ceram. Soc.*, **32**(10) (2004) 1422–1424.
[15] H. P. Zhou, R. L. Fu, L. Chen, H. Chen, R. T. Zhao, *Prog. Nat. Sci.*, **8**(5) (1998) 513–519.
[16] C. Z. Wu, Q. Yang, C. Huang, D. Wang, P. Yin, T. W. Li, Y. Xie, *J. Solid State Chem.*, **177**(10) (2004) 3522–3528.
[17] H. Chen, Y. Cao, X. W. Xiang, *J. Cryst. Growth.*, **224**(3–4) (2001) 187–189.
[18] P. G. Zhang, K. Y. Wang, J. D. Liang, S. M. Guo, *Physica E*, **43**(4) (2011) 934–937.
[19] Z. Q. Shi, M. Radwan, S. Kirihara, Y. Miyamoto, Z. H. Jin, *Ceram. Int.*, **35**(7) (2009) 2727–2733.
[20] P. G. Zhang, K. Y. Wang, S. M. Guo, *Ceram. Int.*, **36**(7) (2010) 2209–2213.
[21] H. T. Cong, H. B. Ma, X. C. Sun, *Physica B*, **323**(1–4) (2002) 354–356.
[22] M. Radwan, M. Bahgat, A. A. El-Geassy, *J. Eur. Ceram. Soc.*, **26**(13) (2006) 2485–2488.
[23] K. Watari, K. Ishizaki, F. Tsuchiya, *J. Mater. Sci.*, **28**(14) (1993) 3709–3714.
[24] H. X. Willems, *J. Eur. Ceram. Soc.*, **10**(4) (1992) 339–346.
[25] X. M. Hou, Z. Y. Yu, Z. Y. Chen, B. J. Zhao, K. C. Chou, *Dalton T.*, **41** (2012) 7127–7133.
[26] W. H. Sutton, A. P. Levitt, Ed., Wiley-Interscience, New York, 1970, pp. 273–342.
[27] W. K. Burton, N. Cabrera, F. C. Frank, *Philos. Trans. R. Soc. Lond.* Ser. **A243** (1951) 299.
[28] R. L. Fu, H. P. Zhou, L. Chen, Y. Wu, *Mat. Sci. Eng. A*, **266** (1999) 44–51.
[29] R. Paul, K. Lee, B. Lee, H. Song, *Mater. Chem. Phys.*, **112**(2) (2008) 562–565.